Attentional modulation of firing rate and synchrony in a model cortical network

Buia Calin (`buia@physics.unc.edu`) and Paul Tiesinga
(`tiesinga@physics.unc.edu`)
Dept. of Physics and Astronomy, University of North Carolina at Chapel Hill

March 2, 2019

Abstract. The response of a neuron in the visual cortex to stimuli of different contrast placed in its receptive field is commonly characterized using the contrast response curve. When attention is directed into the receptive field of a V4 neuron, its contrast response curve is shifted to lower contrast values (Reynolds et al, 2000, Neuron 26:703). The neuron will thus be able to respond to weaker stimuli than it responded to without attention. Attention also increases the coherence between neurons responding to the same stimulus (Fries et al, 2001, Science 291:1560). We studied how the firing rate and synchrony of a densely interconnected cortical network varied with contrast and how they were modulated by attention. The changes in contrast and attention were modeled as changes in driving current to the network neurons. We found that an increased driving current to the excitatory neurons increased the overall firing rate of the network, whereas variation of the driving current to inhibitory neurons modulated the synchrony of the network. We explain the synchrony modulation in terms of a locking phenomenon during which the ratio of excitatory to inhibitory firing rates is approximately constant for a range of driving current values. We explored the hypothesis that contrast is represented primarily as a drive to the excitatory neurons, whereas attention corresponds to a reduction in driving current to the inhibitory neurons. Using this hypothesis, the model reproduces the following experimental observations: (1) the firing rate of the excitatory neurons increases with contrast; (2) for high contrast stimuli, the firing rate saturates and the network synchronizes; (3) attention shifts the contrast response curve to lower contrast values; (4) attention leads to stronger synchronization that starts at a lower value of the contrast compared with the attend-away condition. In addition, it predicts that attention increases the delay between the inhibitory and excitatory synchronous volleys produced by the network, allowing the stimulus to recruit more downstream neurons.

Keywords: attention, synchrony, V4 area

1. Introduction

Neurons in cat primary visual cortex are orientation selective as they respond with maximal firing rates to a bar of their preferred orientation (Hubel, 1959; Hubel and Wiesel, 1959; Hubel and Wiesel, 1962). The firing rate increases with stimulus contrast (Sclar and Freeman, 1982). In addition, when attention is directed into the receptive field of V2 and V4 neurons, the firing rate in response to a visual stimulus inside

the receptive field increases (Luck et al., 1997; McAdams and Maunsell, 1999). Orientation selectivity is preserved across different values for the contrast and attentional state. A fundamental question of neuroscience is how this invariant tuning is achieved and maintained in local cortical circuits. This requires a more detailed understanding of how the firing rate in cortical circuits is regulated by attention and contrast than is presently available.

The contrast response function (CRF, the neuron's firing rate plotted as a function of luminance contrast) has a characteristic sigmoidal shape (Albrecht and Hamilton, 1982; Ohzawa et al., 2002; Sclar and Freeman, 1982; Albrecht et al., 2002). In a study of the attentional modulation of the CRF of V4 neurons it was found that the sensitivity of neurons was increased (contrast gain modulation), because the CRF was shifted to the left (Reynolds et al., 2000; Reynolds and Desimone, 2003). Thus, the neurons were activated by low contrast stimuli to which they did not respond when attention was directed away from the neuron's receptive field. For high enough contrast, the local field potential had a broad peak in the gamma-frequency range (30-80 Hz) (Gray and Viana Di Prisco, 1997; Henrie and Shapley, 2005), suggesting that the cortical network in which the neuron is embedded oscillates in the gamma-frequency range. Likewise, when stimuli were presented that drove the cell strongly, attention increased the correlations between cells responding to similar stimuli and only weakly increased the neuron's firing rate (Fries et al., 2001; Bichot et al., 2005). These results provide support for the idea that the effects of attention on firing rate and neural synchrony are equivalent to changing the effective contrast of the stimulus. Despite these similarities, it is not clear whether attention and contrast use the same mechanism to modulate the neuron's responses. Nor is it clear whether contrast and attention act similarly on the correlations between neurons.

The response of a single neuron model to temporally patterned excitatory and inhibitory synaptic inputs was studied previously (Tiesinga et al., 2004b). Attention was postulated to alter the precision of presynaptic spike trains (Tiesinga et al., 2004b). The model did not offer a mechanistic explanation for how these changes could occur. Here, we study attentional modulation of a strongly coupled model network, representative of those in the superficial layers of cortex (Yoshimura et al., 2005). In cat and macaque primary visual cortex, the stimulus orientation that most strongly activates neurons varies systematically with the location on the cortical surface (Blasdel, 1992a; Blasdel, 1992b). Similar, but more elaborate maps are also thought to exist in downstream cortical areas such as V2 and V4 (Ghose and Ts'o, 1997). These maps have not been studied in great detail. Here we study the response of

neurons at one particular cortical location to a stimulus of the optimal orientation. The basic assumption is that attention and changes in contrast are mediated by changes in driving currents to the excitatory and inhibitory neurons in the network. Our simulation results reveal that increasing the drive to excitatory neurons has a different effect than decreasing the drive to inhibitory neurons. Specifically, varying the driving current to the interneurons leads to synchrony modulations by way of so called locking steps. We explore whether it is possible to account for the experimental results under the hypothesis that contrast drives the excitatory neurons more strongly than the inhibitory neurons and that attention leads to a reduction in the drive to the inhibitory neurons.

2. Methods and model description

2.1. Model summary

We use a generic network model that is an approximation for local networks in V1, V2 and V4. We focus our attention on a subnetwork of strongly interconnected neurons, based on observations made in layer 2/3 of rat primary visual cortex made by (Yoshimura et al., 2005). The model consisted of four hundred excitatory pyramidal neurons and a hundred inhibitory interneurons (Figure 1). In the model used for the initial exploration, the neurons were connected all-to-all with inhibitory $GABA_A$ synapses and excitatory AMPA synapses. For the robustness part of the study a sparsely coupled network was used. In addition to the excitatory and inhibitory inputs from other neurons in the subnetwork, the neurons also received feed-forward stimulus-related excitatory inputs ("contrast"), modulatory top-down inputs ("attention") and inputs from other neurons in the same layer, which are not part of the simulated network. All of these inputs were modeled as a time varying current, the mean of which was I_{exc} (I_{inh}) and the variance of which was λ_{exc} (λ_{inh}) for excitatory (inhibitory) cells. We used Hodgkin-Huxley-type model neurons for excitatory pyramidal cells (Golomb and Amitai, 1997) and for inhibitory interneurons (Wang and Buzsaki, 1996). A full description of the single neuron model equations, the synapse models, and details regarding computational implementation are given in the appendix. In summary, the key parameters varied in the simulation were: the driving current I_{exc} (I_{inh}), the current-noise strength λ_{exc} (λ_{inh}), and the heterogeneity parameters σ_{exc} (σ_{inh}) for excitatory (inhibitory) neurons as well as the synaptic coupling parameters (g_{ee}, g_{ei}, g_{ie}, g_{ii}), defined as the unitary
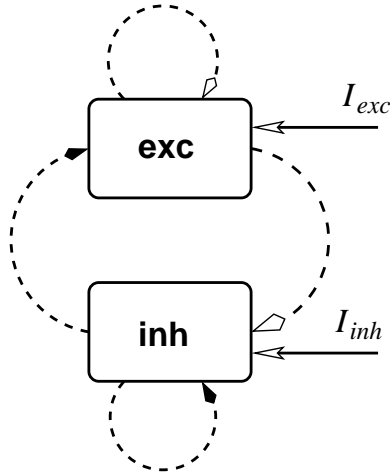
Figure 1. The model network consisted of a fully connected set of excitatory and inhibitory neurons. Each excitatory and inhibitory neuron also received a constant driving current equal to I_{exc} and I_{inh}, respectively.

synaptic strength times the number of inputs to the receiving neuron. The subscript "*ie*" stands for the inhibitory input to the excitatory neurons, with an analogous interpretation for "*ii*", "*ee*" and "*ei*". Driving currents and heterogeneity are expressed in $\mu A/cm^2$, noise strength in mV^2/ms and synaptic strength in mS/cm^2.

We performed many exploratory simulations. For almost all combinations of synaptic coupling parameters that were studied, we found values for the excitatory and inhibitory driving current for which the network was in a synchronous state. Not all of these states were equally robust against noise and heterogeneity. (Borgers and Kopell, 2003; Borgers and Kopell, 2005; Borgers et al., 2005) report on procedures for finding coupling parameters that yield robust synchronization. The authors suggest that the loss of synchrony proceeds either by "phase walkthrough", for which the interneurons receive enough driving current and tonic excitatory synaptic inputs to spike without having to wait for synchronous excitatory inputs, or via "suppression", for which the interneurons fire at such a high rate or at such a low degree of synchrony that they prevent the excitatory neurons from firing. They also note that asynchronous interneurons are more effective in suppressing excitatory cells than synchronous interneurons firing at the same rate. To obtain robust synchrony (Borgers and Kopell, 2003; Borgers and Kopell, 2005; Borgers et al., 2005): (1) the current drive to the interneurons should be low enough that synchronous excitatory synaptic inputs are necessary for spiking, in order to prevent phase walkthrough; (2) the ratio of the inhibitory synaptic current to excitatory neurons

over the excitatory synaptic current should be large enough to ensure robustness, but small enough to prevent suppression. We picked for further analysis the following set of coupling parameters (g_{ee}, g_{ei}, g_{ie}, g_{ii})= (0.05, 0.15, 0.15, 0.15) consistent with these requirements. The parameter (λ_{exc}, λ_{inh}) took two values: (0.02, 0.1) and (0.2, 0.6), corresponding to low and high noise states, respectively. The heterogeneity parameters were $\sigma_{exc} = 0.1$ and $\sigma_{inh} = 0.02$.

To test the robustness of our findings for the all-to-all network, we performed simulations of a network with sparse synaptic connections, high noise levels and large heterogeneities in the drive to the excitatory cells. All connections were made stochastically with a probability of 20% (Brunel and Wang, 2003), with the exception of the recurrent inhibitory connections, which remained all-to-all. The synaptic coupling strengths were made stronger, $g_{ee} = 0.1$ (80), $g_{ei} = 0.5$ (80), $g_{ie} = 0.3$ (20) and $g_{ii} = 0.5$ (100). The number between the parentheses indicates the average number of connections the neuron received. A hundred excitatory cells (referred to as the top-100) received a driving current I_{exc} with an offset varying linearly from 0.5 for the first neuron to - 0.5 for the hundredth neuron; the remaining three hundred (referred to as the bottom-300) received a driving current $I_{exc} - 1$, also with a linear offset between -0.5 and 0.5. Note that highest current for the bottom-300 is equal to the lowest current for the top-100. The current to the inhibitory neurons was normally distributed with mean I_{inh} and a standard deviation of $\sigma_{inh} = 0.1$. The voltage noise variances are $\lambda_{exc} = 0.1$ and $\lambda_{inh} = 0.5$.

2.2. ANALYSIS

The spike time was defined as the time at which the membrane potential crossed a threshold value from below. The threshold value was taken to be 0 mV for interneurons and -20 mV for pyramidal neurons. The mean firing rate was calculated as the inverse of the mean interspike interval for each neuron, averaged over all neurons of the same type (i.e. separately for all the inhibitory and all the excitatory neurons):

$$r = \frac{1}{N} \sum_i \left(\frac{1}{n^i - 1} \sum_j (t_{j+1}^i - t_j^i) \right)^{-1}$$

where t_j^i was the jth spike time of neuron i, n_i was the number of spikes produced by neuron i, and N was the total number of neurons of a given type. In this notation, r_{exc} and r_{inh} were the average firing rates of the excitatory and the inhibitory neurons, respectively. The degree of synchrony of the system was estimated using the coefficient of

variation for a population of neurons, CV_P. This measure of synchrony is based on the idea that during synchronous states the minimum distance between spikes of different neurons is reduced compared with asynchronous states. First, the spike times of the whole population of neurons were pooled together and sorted in ascending order. The sorted set of aggregate spike times t_j was labeled by the index j. The interspike interval between two consecutive spikes $t_j = t_{j+1} - t_j$ typically involved spikes from two different neurons. The coefficient of variation of the combined interspike intervals is:

$$CV = \frac{\sqrt{\langle \Delta t_j^2 \rangle - \langle \Delta t_j \rangle^2}}{\langle \Delta t_j \rangle}$$

Here $\langle \bullet \rangle$ was the average across all intervals j. The value of the CV is one for an asynchronous network (Tiesinga and Sejnowski, 2004), whereas for a perfectly synchronous network it is approximately $\sqrt{N}$ (Tiesinga and Sejnowski, 2004), with N being the number of active neurons in the network. In the model, there were four times as many excitatory neurons as there were inhibitory neurons. Hence, in order to compare the synchrony of the excitatory neurons to that of the inhibitory neurons, we subtract one from the CV, and, in addition, divide it by $\sqrt{N_{exc}/N_{inh}} = 2$ for the excitatory neurons. The resulting quantity is denoted by CV_P (this is different from the normalization used previously in (Tiesinga and Sejnowski, 2004)). A CV_P value close to zero then corresponds to an asynchronous state, while a value greater than zero indicates synchrony; the higher the synchrony, the higher the CV_P is. There are two different aspects of synchrony: the degree of coincidence and the level of precision. The CV_P confounds coincidence and precision (Tiesinga and Sejnowski, 2004). Specifically, for a synchronous network in which the neurons fire only once every few cycles, but when they do so at high precision, the CV_P can have a value comparable to that of a network where neurons fire every cycle but at a lower precision. The delay between inhibitory and excitatory volleys was determined based on the interspike interval (ISI) distribution. For each interneuron spike, we first determined all the ISIs with a given excitatory neuron. We only keep the ISI with the smallest absolute value and then repeat this procedure for all excitatory neurons and across all interneuron spikes. This yields $N_{inh}^{sp} \times N_{exc}$ interspike intervals, where N_{inh}^{sp} was the total number of inhibitory spikes and N_{exc} was the number of excitatory neurons. The distribution of ISIs had at least one peak when the network was synchronized. The location of the peak closest to zero ISI was taken as an estimate of the delay between

the excitatory and inhibitory spike volleys. This delay could be positive or negative. Spike time histograms (STH) were obtained as

$$STH = \frac{1000\Delta t}{N} \sum_{i=1}^{N} X_i(t)$$

where

$$X_i(t) = \begin{cases} 1, & \text{if } t_j^i \in (t - \Delta t/2, t + \Delta t/2) \\ 0, & \text{otherwise} \end{cases}$$

$N = N_{exc}$ or N_{inh} was the number of neurons of a given type and the bin width was $\Delta t = 2$ ms.

The frequency, f_{osc}, of the network oscillation was determined as the location of the highest peak in the Fourier transform of the interneuron spike time histogram.

3. Results

Our goal is to characterize first how synchrony and firing rate are modulated in cortical networks (Figure 2 to 6), and then link these simulation results to the observed effects of attention on the contrast response function (Figure 7 to 9). When the driving current to the excitatory cells is increased, their firing rate increases. Recurrent excitatory connections cause a larger excitatory drive to both the excitatory neurons as well as the inhibitory neurons. Hence, the excitatory cells also receive more inhibition. The net increase in the firing rate of the excitatory and the inhibitory neurons will depend on how much inhibition is recruited, which is proportional to both g_{ei} and g_{ie}. What would happen if the driving current to the inhibitory cells was increased instead? The rate of the inhibitory neurons would initially increase, but that increase would reduce the firing rate of the excitatory neurons, and the rate of excitatory inputs to the interneurons as well. The net increase in the interneuron firing rate and the decrease in the firing rate of the excitatory neurons again depends on the relative strength of g_{ei} and g_{ie}. The preceding analysis is based only on the changes in firing rate. However, there may also be changes in synchrony that could lead to an increase or a reduction in the effectiveness of the synaptic inputs in making the postsynaptic cells spike (Salinas and Sejnowski, 2000; Tiesinga et al., 2004a).
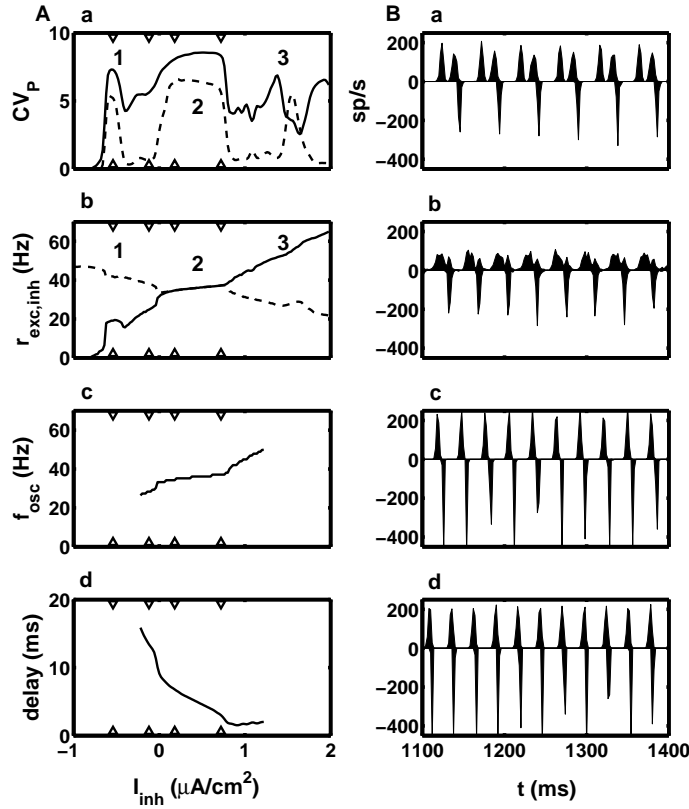
Figure 2. Network synchrony and the delay between inhibitory and excitatory volleys were modulated by the inhibitory driving current. (A) We plot as a function of the inhibitory driving current I_{inh}, (a) CV_P for the excitatory (dashed line) and the inhibitory neurons (solid line), (b) the firing rate of the excitatory (dashed line) and inhibitory neurons (solid line), (c) the oscillation frequency when the network is in or near a 1:1 locking state, (d) the delay between the inhibitory volley and the excitatory volley. (B) In each panel, we plot the spike time histogram for the excitatory neurons (positive rates) and inhibitory neurons (negative rates). The driving currents used in (a) to (d) correspond to the currents indicated by the open triangles in A, from left to right, respectively. The numbers in Aa and Ab are described in the main text. The driving current to the excitatory neurons was $I_{exc} = 3.94 \, \mu\text{A/cm}^2$ and we used a low noise level.

3.1. Variation of the drive to the inhibitory neurons.

Synchrony modulations lead to so called $n : m$ locking steps, during which n synchronous excitatory volleys are followed by m synchronous inhibitory volleys (here either n or m is one). In Figure 2 we show the behavior of the all-to-all network at a low noise level. Three locking

steps are visible, the 2:1, 1:1 and 1:2 steps, labeled by 1, 2 and 3, respectively (Figure 2Aa and 2Ab). On the locking steps the network was highly synchronous, as quantified by the CV_P (Figure 2Aa), and the excitatory and inhibitory firing rates varied little with I_{inh} (Figure 2Ab). On the 1:1 step, the excitatory and inhibitory firing rates were equal to the oscillation frequency (Figure 2Ac). In addition, the delay between inhibitory and excitatory volleys decreased monotonically from 6.78 ms at the lowest current value on the step to 3.01 ms at the highest current value on the step. The histograms of the corresponding network activity are shown in Figure 2Bb and 2Bc, respectively. A reduction in synchrony by way of the phase walkthrough mechanism (Borgers and Kopell, 2005) was signaled by the delay approaching zero. During phase walkthrough the interneurons receive enough driving current to be able to spike without having to wait for synchronous excitatory volleys. The reduction in synchrony induced by increasing I_{inh} on the 1:1 step led to an increase in inhibitory firing rate, whereas on the 2:1 step it led to a decrease (Figure 2Ab). The former is expected in view of the increased inhibitory driving current, the latter is the exception. [1]

In Figure 3 we show the behavior of the same network but at high noise levels. Only the 1:1 step remained. It was characterized by a peak in the CV_P (Figure 3A), but, in contrast to the results for a low noise level, the excitatory and inhibitory rate were not exactly equal because the interneuron skipped oscillation cycles (Figure 3B). However, as before, the delay between inhibition and excitation decreased systematically with I_{inh} (Figure 3C). Outside the 1:1 step the network is asynchronous, with CV_P values close to zero (Figure 3A). These results show that a low noise strength is not a necessary condition for the presence of 1:1 locking states and modulation of synchrony and delay with interneuron drive.

In summary, due to the presence of locking states, the rate of increase of r_{inh} and the rate of decrease of r_{exc} with inhibitory driving current varied non-monotonously, and large modulations in the degree of synchrony were obtained.

---

[1] This comes about as follows. For I_{inh} values below the onset of the 2:1 step, the asynchronous excitatory synaptic inputs to the interneurons were below threshold. Only synchronized excitatory volleys, with approximately the same number of excitatory spikes, could elicit spikes from the interneurons. Hence, the onset of the 2:1 step was associated with a sharp increase in inhibitory rate. In contrast, when the step became unstable, the asynchronous excitation was less efficient in driving the interneurons than the synchronous volleys were on the locking step, yielding a sharp reduction in firing rate.
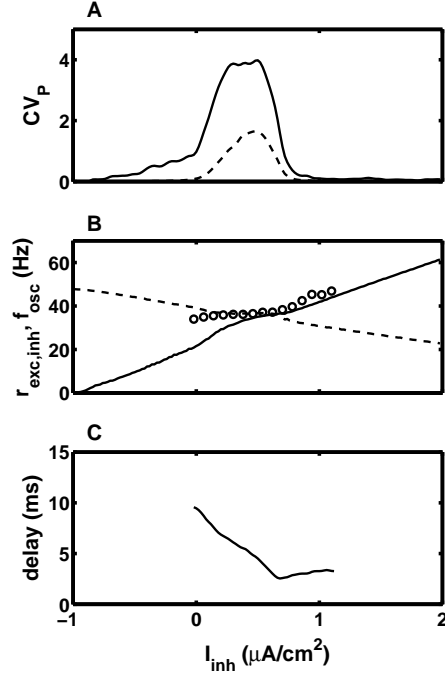
Figure 3. For high noise levels, synchrony only occurred for a limited range of driving currents. We plot, (a) CV_P for excitatory (dashed line) and inhibitory neurons (solid line), (b) the firing rate of excitatory (dashed line) and inhibitory neurons (solid line) and the oscillation frequency (open circles), (c) the delay between inhibition and excitation. The quantities are plotted as a function of the inhibitory driving current I_{inh}. The simulations were performed for a high noise level with $I_{exc} = 3.94\,\mu\mathrm{A/cm}^2$.

3.2. Variation of the drive to the excitatory neurons.

When the drive to the inhibitory neurons was increased, the inhibitory rate increased whereas the excitatory rate decreased. Therefore, irrespective of what the initial firing rate of the excitatory neurons was, there would be an inhibitory driving current for which the inhibitory and excitatory rates would be approximately equal, so that there could be locking steps. When the excitatory current is increased, both the excitatory as well as inhibitory rates increase. Therefore the two rates do not necessarily converge to each other. We investigate two regimes based on the value of the driving current to the inhibitory cells.

First, for a weak depolarizing drive to the interneurons ($I_{inh} = 0.38$, Figure 4A), the excitatory and inhibitory firing rates were comparable at the start of the interval over which excitatory current was varied. Initially, the inhibitory cells fired at twice the rate of the excitatory cells, but eventually the excitatory and inhibitory rates became equal,
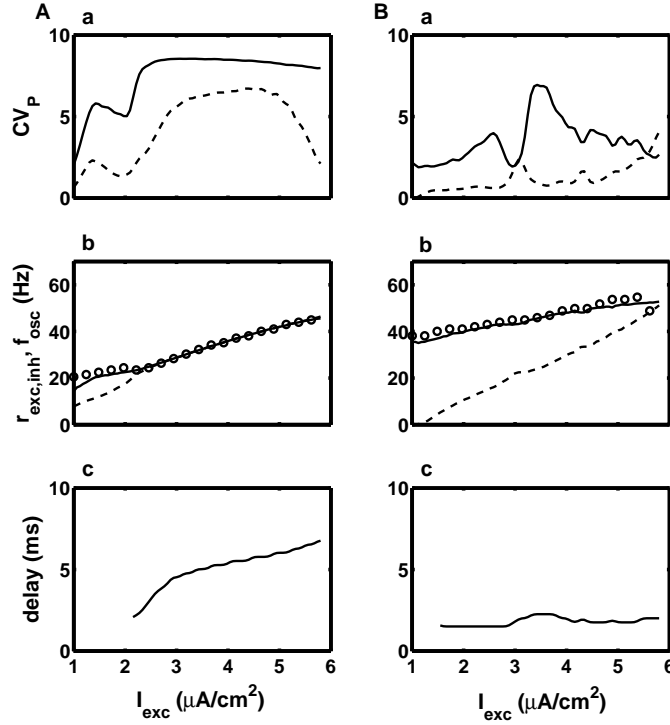
Figure 4. (A) For a small depolarizing current to the interneuron network, synchronous states were obtained for a wide range of excitatory driving currents. We plot as a function of the excitatory driving current I_{exc}, (a) CV_P for the excitatory (dashed line) and the inhibitory neurons (solid line), (b) the firing rate of the excitatory (dashed line) and the inhibitory neurons (solid line) and the oscillation frequency (circles), (c) the delay between inhibition and excitation. (B) For a high depolarizing current to the interneuron network, synchrony resonances were observed. Panels are as in (A). The driving current to the inhibitory neurons was $I_{inh} = 0.38\,\mu\mathrm{A/cm}^2$ for (A) and $I_{inh} = 1.18\,\mu\mathrm{A/cm}^2$ for (B) and we used a low noise level.

at which point the network fully synchronized (Figure 4Aa). The synchronous state was very stable against increases in driving current, yielding a range of firing rates from 25 to 45 Hz for which the network was synchronized (Figure 4Ab). The delay went from about 2.26 ms at the start to 6.53 ms at the end of the locking step (Figure 4Ac). [2]

---

[2] As mentioned before, the loss of synchrony proceeds via a phase walkthrough mechanism, signaled by the vanishing of the delay between inhibitory and excitatory volleys. The region in the $I_{exc}-I_{inh}$ parameter plane for which 1:1 locking is obtained has a shape that resembles the inside of an ellipse. The long axis is closer in direction to the I_{exc} axis, whereas the short axis is more parallel to the I_{inh} axis. This means that it is easier to leave the locking step by varying I_{inh} compared with varying

Second, for a strong depolarizing drive ($I_{inh} = 1.18$, Figure 4B), the interneurons fired at a much higher rate than the excitatory cells. The CV_P value for the excitatory neurons was less than for the interneurons (Figure 4Ba). However, this was due to their low firing rate: when the excitatory neurons fired on an oscillation cycle they did so at high precision (see Methods). There was a local increase in the interneuron coherence when the oscillation frequency was around 45Hz, indicating a preference for oscillations in the middle of the gamma-frequency range. In this state, the excitatory neurons were mainly following the inhibitory rhythm, smoothly increasing their rate with driving current (Figure 4Bb). In addition, the delay was virtually constant over the entire current range (Figure 4Bc).

Thus, in general, delay modulations are reduced when the drive to the excitatory neurons is varied compared with when the drive to the interneurons is varied. In addition, on the locking step, the inhibitory and excitatory rates vary with the excitatory driving current, but their ratio is constant.

3.3. ROBUSTNESS OF LOCKING STATES IN SPARSE AND HETEROGENEOUS NETWORKS

The results presented in the preceding sections were obtained using an all-to-all connected network with small heterogeneities in the driving currents. Because the degree of heterogeneity was so small, we refer to this network as the homogenous, all-to-all network. Cortical networks are characterized by a sparse synaptic connectivity and heterogeneity in neural properties (Binzegger et al., 2004; Shepherd et al., 2005; Song et al., 2005). Furthermore, during synchronous states in vivo, neurons might not fire on each cycle of the oscillation (Fries et al., 2001). We therefore explored whether there are locking states in sparsely coupled, heterogeneous networks for which the mean inhibitory and excitatory firing rate is less than the oscillation frequency and whether in these states the delay between inhibitory and excitatory volleys could still be modulated by the driving current to the inhibitory neurons. The parameter space for this model network was much larger than for the homogeneous, all-to-all network. The additional parameters include the degree of sparseness and the dispersion of driving currents across network neurons. Therefore, we did not attempt a systematic study of the entire parameter space, rather we report on the results obtained

---

I_{exc}. As a result the rate of change in delay with I_{inh} is also larger. Whether the delay on the 1:1 locking step increases or decreases with increasing I_{exc} depends on whether I_{exc} moves away from, or closer to, the high I_{inh} edge of the locking region. For the parameter values used in Figure 4A, the delay increased.

with two representative parameter sets. For these sets, small changes in parameter settings did not result in qualitative changes in the network states, indicating that the behavior we found was robust. The first parameter set was adjusted to obtain network states with mean firing rates that were much less than the oscillation frequency. The coupling constants were $(g_{ee}, g_{ei}, g_{ie}, g_{ii}) = (0.1, 0.5, 0.3, 0.5)$. The second parameter set was tuned such that the excitatory rates were between 15 and 35 Hz in order to reproduce the CRFs measured by (Reynolds et al., 2000). This was accomplished by reducing the strength of the inhibitory synapses onto the excitatory neurons from $g_{ie} = 0.3$ to 0.2. The excitatory neurons in the network were divided into two groups (see Methods), a hundred neurons with a high driving current (because the stimulus matched the preferred stimulus feature of the neurons), and three hundred neurons with a lower driving current (because stimulus did not exactly match the neurons' preferred stimulus feature). These neurons are referred to as the top-100 and bottom-300, respectively. For set 1, oscillation frequencies between 22 and 50 Hz were obtained, whereas set 2 yielded a range between 25 and 60 Hz.

The 1:1 locked states in the sparse, heterogeneous networks consisted, as before, of an excitatory volley followed by an inhibitory volley (Figure 5Ba, parameter set 2). These synchronous states arose via a robust version of the mechanism observed in the homogeneous, all-to-all network. The parameters were tuned such that a synchronous volley, in which only a fraction of the excitatory neurons participated, could elicit a synchronous inhibitory volley. The less excitable neurons could fire between the initial excitatory volley and the recruited inhibitory volley. This implies that the firing rate of the bottom-300 should depend on the value of the delay between the inhibitory and initial excitatory volley (Figure 5Ad). Indeed, there was a range of I_{inh} values for which the rate of the top-100 neurons increased (data not shown) or remained approximately constant (Figure 5Ac), but the rate of the bottom-300 (Figure 5Ac) and the delay decreased (Figure 5Ad). During moderately synchronous states, the top-100 neurons typically had firing rates below, but relatively close to, the oscillation frequency with a broad dispersion ($I_{inh} = 0.93$, $I_{exc} = 3.5$, Figure 5Bb). The bottom-300 (Figure 5Bc) and the inhibitory neurons (Figure 5Bd) had rates that were generally much lower than f_{osc}. For this particular example, they took values between approximately 4 and 23 Hz and between 4 and 34 Hz, respectively, with f_{osc} being approximately 37 Hz. For parameter set 1, even larger differences between the oscillation frequency and the mean firing rate were obtained (data not shown). For highly synchronous states (example: parameter set 2, $I_{inh} = 0.27$, $I_{exc} = 4.75$), a large fraction of the top-100 fired at the oscillation
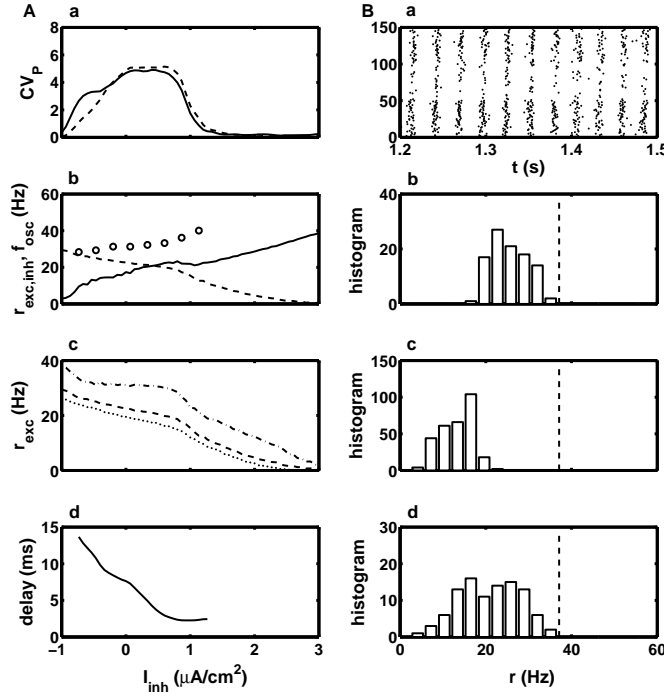
Figure 5. Locking states in sparse, heterogeneous networks. In panel A, we plot as a function of I_{inh}, (a) the degree of synchrony (CV_P) for excitatory (dashed line) and inhibitory neurons (solid line); (b) the oscillation frequency (fosc, open circles), mean firing rate across all excitatory (dashed line) and inhibitory neurons (solid line); (c) mean firing rate across the top-100 (dot-dashed line), the bottom-300 (dotted line) and all excitatory neurons (dashed line); (d) the delay between inhibitory and the initial (top-100) excitatory volley. (B) The locked-state for $I_{inh} = 0.93\,\mu\text{A/cm}^2$. (a) Rastergram, with, from top to bottom, 50 spike trains from the inhibitory neurons, 50 spike trains from the bottom-300 and 50 spike trains from the top-100 excitatory neurons. Histograms of the distribution of firing rates across network neurons for (b) the top-100, (c) the bottom-300 excitatory neurons and (d) the inhibitory neurons. The dashed vertical line in (b-d) indicates the oscillation frequency. Data was obtained from a sparse, heterogeneous network with parameter set 2 with $I_{exc} = 3.5\,\mu\text{A/cm}^2$.

frequency, with the bottom-300 firing at a lower rate and at a significant delay (data not shown). In that case, the firing rate of the most depolarized excitatory neurons determined the oscillation frequency. Thus, it is the subsystem consisting of the top-100 excitatory neurons and the interneurons, which shows behavior similar to that obtained in the homogeneous, all-to-all network. The main difference is that the overall excitatory and inhibitory firing rate can be different from
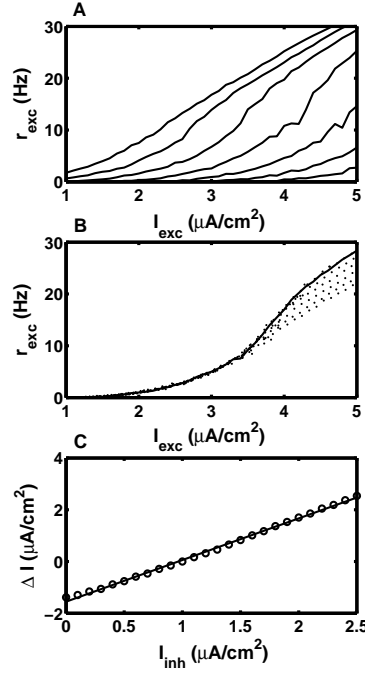
Figure 6. The inhibitory driving current modulates the sensitivity of the $r_{exc} - I_{exc}$ curves. (A) $r_{exc} - I_{exc}$ curves for, from top to bottom, $I_{inh} = 0.05, 0.45, 0.85, 1.25, 1.65, 2.05,$ and 2.45 μA/cm^2. (B) The same curves, but now each curve is shifted over a distance $\Delta I(I_{inh})$, chosen to make the curves as similar as possible to a reference curve with $I_{inh} = 1.0$. (C) Shift distance $\Delta I(I_{inh})$ as a function of the inhibitory driving current. Data was obtained from a sparse, heterogeneous network with parameter set 1.

the oscillation frequency (Brunel and Hakim, 1999; Brunel and Wang, 2003; Geisler et al., 2005) and that the states are much more robust against heterogeneity.

We also investigated how the $r_{exc} - I_{exc}$ curves depended on the inhibitory driving current (Figure 6A, parameter set 1). In general, there were two regimes in the $r_{exc} - I_{exc}$ curve. For low firing rates, r_{exc} varied as a power of I_{exc}, $r_{exc} = 0.3(I_{exc} - B)^A$ (Hansel and van Vreeswijk, 2002; Miller and Troyer, 2002), here A and B are fitting parameters. A is approximately independent of I_{inh}, $A = 3.2 \pm 0.1$, the "shift" B is discussed below. For higher firing rates, the rate of change of r_{exc} with I_{exc} first increased, but decreased soon after that, when the firing rate reached saturation. The low firing rate (power law) portion of the curves could be made to fall on top of a reference curve ($I_{inh} = 1.0\,\mu$A/cm^2) by shifting them over a distance ΔI along the I_{exc}
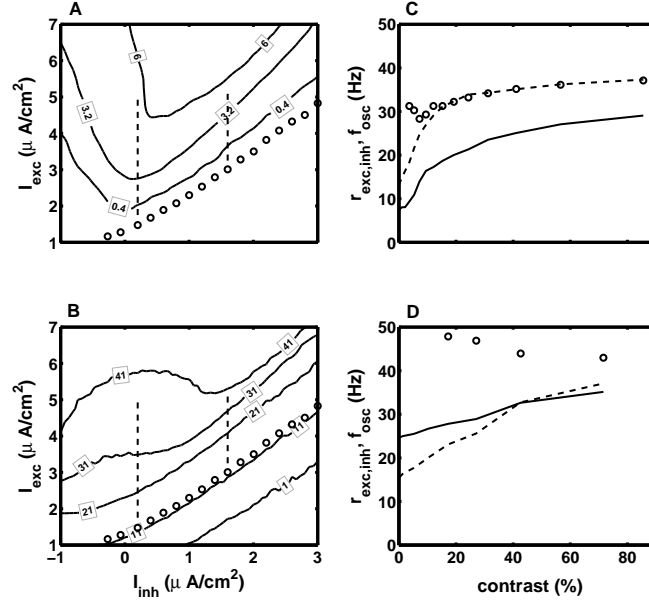
Figure 7. A-B: The trajectory in $I_{exc} - I_{inh}$ space obtained by varying contrast. We plot the contour lines (solid lines) for (A) the inhibitory CV_P and (B) the excitatory firing rate for the top-100 neurons. In each panel we also show the lines of varying contrast for a fixed level of attentional modulation (dashed lines) and the line corresponding to zero contrast and varying attentional condition (circles). C-D: In each panel, we plot as a function of contrast, the firing rate of the top-100 excitatory (dashed line) and inhibitory neurons (solid line) as well as the oscillation frequency (open circles), We show the model response when attention is (C) directed into the receptive field and (D) when it is directed away from the receptive field. Data was obtained from a sparse, heterogeneous network with parameter set 2.

coordinate (Figure 6B). This means that $B \approx \Delta I(I_{inh}) + 1$. The shift ΔI was a linear function of I_{inh} (Figure 6C, slope=1.6, y-intercept: -1.6 μA/cm^2). For parameter set 2, the shifts were present for a smaller range of inhibitory current values, but the curves overlapped for higher firing rates of up to 20 Hz (results not shown). These results are a proof of principle that the sensitivity of the network activity can be modulated via the inhibitory driving current.

3.4. CONTRAST AND ATTENTION DEPENDENCE OF THE CORTICAL RESPONSE

The contrast-response function measured in experiments is represented by the firing rate of the excitatory neurons in the network. Experimental measurements of the CRF in LGN and V1 can be fit by the rela-

tionship (Albrecht and Hamilton, 1982; Sclar and Freeman, 1982; Alitto and Usrey, 2004):

$$f(c) = f_m \frac{c^n}{c_0^n + c^n}$$

Here f_m is the firing rate at saturation, c is the stimulus contrast, c_0 is the contrast for which the firing rate is half the saturation rate, and n can be interpreted as a steepness parameter. Strong contrast saturation effects are already present in neurons in LGN, V1 and V2, that provide direct or indirect inputs to V4. Therefore, we do not have to fully account for saturation effects in the network model; rather, we assume that the driving currents, which represent the feed forward inputs, vary with contrast according to $f(c)$. We took an $f(c)$ appropriate for LGN inputs from (Troyer et al., 1998): $c_0 = 13.3\%$, $n = 1.2$, $f_m = 53$ Hz. As an additional simplification, we assume that the driving currents are a linear combination of the CRF $f(c)$ and the attentional state a. That is:

$$\begin{bmatrix} I_{exc}(c,a) \\ I_{inh}(c,a) \end{bmatrix} = \begin{bmatrix} I_{exc0} \\ I_{inh0} \end{bmatrix} + \begin{bmatrix} A_{11} & A_{12} \\ A_{21} & A_{22} \end{bmatrix} \begin{bmatrix} f(c) \\ a \end{bmatrix}$$

Presently, the coefficients in the matrix are not known to sufficient detail. For instance, we do not know what is the relative increase in drive to excitatory neurons with contrast compared with the increase in drive to inhibitory neurons. By the same token, we do not know whether attention, which could potentially be mediated by either cholinergic or glutamatergic projections (Hasselmo and McGaughy, 2004; Coull, 2005; Milstein et al., 2005; Sarter et al., 2005), affects the interneurons more strongly than the excitatory neurons. These coefficients were therefore treated as free parameters. There is also a baseline current, I_{exc0} and I_{inh0}, in order to get excitatory rates close to 15 Hz for zero contrast (corresponding to a gray screen (Reynolds et al., 2000)). We report results based on one choice of parameter values: $I_{exc0} = 3.007$, $I_{inh0} = 1.600$, $A_{11} = 0.0898$, $A_{12} = -1.532$, $A_{21} = 0$, $A_{22} = -1.400$. A_{21}/A_{11} is the ratio between contrast-induced current to interneurons over that to excitatory cells. In the present case it is zero, implying that interneurons are not affected by the amount of contrast. However, similar results were found for ratios between -0.15 and 0.20.

The network responses were calculated on a two-dimensional grid of I_{inh} and I_{exc} values. We used data obtained from simulations of the sparse, heterogeneous network with parameter set 2. The firing rate was averaged across the top-100 neurons, since these were the neurons most strongly activated by the stimulus. Then we constructed the responses as a function of c for a given value of "attentional modulation", a.
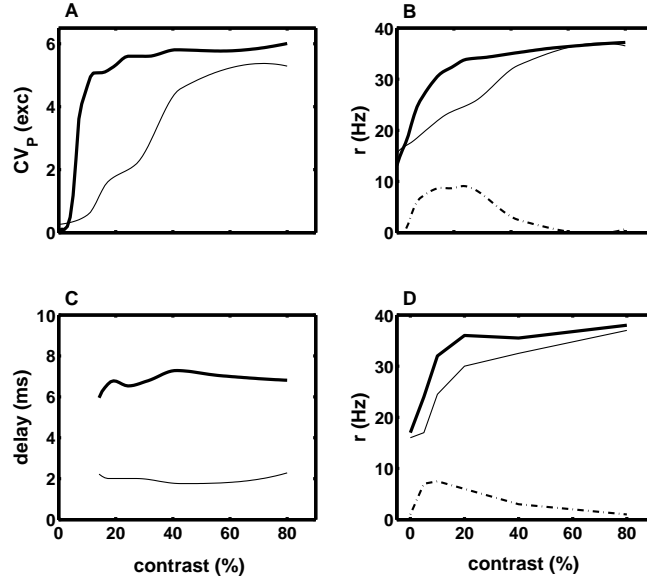
Figure 8. Comparison of the response of the top-100 excitatory neurons between the attend-into-the-receptive-field (thick solid lines) and the attend-away condition (thin lines). We plot as a function of contrast, (A) the CV_P, (B) the firing rate, (C) the delay between inhibition and excitation. In (D) we reproduced the experimental data shown in Figure 5 of (Reynolds et al., 2000). Simulation data were the same as in Figure 7.

Here the "attentional modulation" could take only two values: $a = 0$ for the attend-away state, and $a = 1$ for the attend-into-RF state. As c is varied, a line is traced out in $I_{exc} - I_{inh}$ space. The rate at which the line is traced out with contrast is not uniform because of the saturation, $f(c)$. In Figure 7A and B, we show the line for the attend-away condition and to the left of it (at lower I_{inh} values), the line for when attention is directed into the neuron's receptive field. The starting point of each line corresponds to zero contrast for the particular attentional condition. The starting points lie on a line characterized by constant c and varying a. There have been experiments in which attention increased the spontaneous activity, whereas in other experiments no significant changes were observed (Moran and Desimone, 1985; Luck et al., 1997). Here, the parameters of this line were chosen so that the firing rate at zero contrast is approximately independent of attentional state.

For weak contrast, in the attend-away condition, interneurons fired at about 25 Hz, whereas the excitatory neurons had a much lower firing rate (Figure 7D). As the contrast was increased, the excitatory

rate increased significantly, whereas the inhibitory rate increased at a much lower rate. At approximately 50% contrast, the excitatory and inhibitory rate became quite similar, and the degree of synchrony in the gamma-frequency range increased (Figure 8A). The delay between inhibition and excitation remained approximately constant during this manipulation (Figure 8C). The effect of attention was modeled as a decrease in driving current to the inhibitory neurons. With attention, the excitatory firing rate increased much faster with increasing contrast and saturated for lower values of contrast (approximately 20%, Figure 7D), synchrony was obtained at a lower contrast as well (Figure 8A). The degree of synchrony, as quantified using the CV_P, was significantly higher with attention for contrast values up to 60% (Figure 8A). Even for higher contrast, when the firing rates for both conditions were approximately the same, there still was a small difference in CV_P values. During the synchronous state, with attention into the receptive field, the delay between excitation and inhibition was higher than in the attend-away condition (Figure 8C). The magnitude of the attentional modulation of firing rate in the model (Figure 8B) is similar to that obtained in the experiments by (Reynolds et al., 2000) which were reproduced in Figure 8D. For the experimental as well as the computational results, the saturation firing rate was not affected by the attentional condition, indicating that the effect of attention is more consistent with a shift in sensitivity than a change of gain. However, the CRF curves themselves are not exactly shifted versions of each other. In the model, we obtained shifts in sensitivity by modulating the inhibitory driving current (Figure 6).

3.5. Delay between inhibition and excitation affects downstream neurons.

We also determined how changes in network state might affect downstream neurons. For the present investigation, we assumed that the downstream neuron received excitatory and inhibitory inputs from the network. This means that it is local, because connections between different cortical areas are predominantly excitatory (Salin and Bullier, 1995). We are considering the effect of the vertical projection from layer 4 to layer 2/3 and from layer 2/3 to layer 5, rather than the long-range horizontal projections that link different microcolumns (Callaway, 1998; Douglas and Martin, 2004) The downstream neuron was modeled in the same way as an excitatory neuron in the network, with a driving current $I = -0.5$ (in $\mu A/cm^2$), a total excitatory input conductance of 0.6 (in mS/cm^2, 400 inputs) and a total inhibitory conductance of 0.15 (100 inputs). We ran the homogeneous, all-to-all
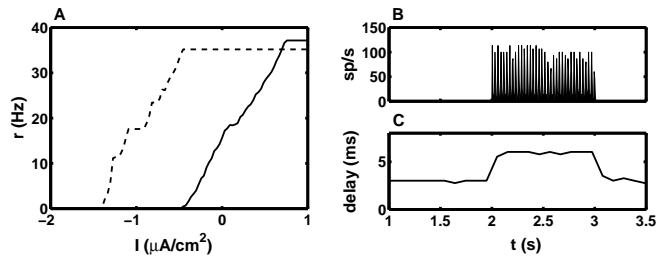
20

Figure 9. Downstream neurons were sensitive to the delay between inhibition and excitation. (A) We plot the firing rate of a downstream neuron for a small delay between inhibition and excitation ($\Delta t = 3.01$ ms, solid line) and a larger delay ($\Delta t = 6.03$ ms, dashed line). (B) When the delay was dynamically switched from the low value (at $t < 2000$ ms) to the higher value (during the interval $2000 < t < 3000$ ms), the neuron's firing rate increased instantaneously. We plot the spike time histogram for the responses of a single downstream neuron across 20 trials. (C) Time evolution of the delay for the network used as input in (B).

network for an extended period of time for two different values of the inhibitory driving current (parameters as in Figure 2, with $I_{exc} = 3.94$, $I_{inh} = 0.72$ and 0.28, respectively). For both values the network was synchronized. In addition, for both states, the oscillation frequency, the excitatory firing rate and inhibitory firing rate were also approximately equal. Only the delay was significantly different. The firing rate of the downstream neurons was increased strongly when the network delay was increased (Figure 9A,B). The firing rate versus driving current curve was shifted to the left when the delay was increased (Figure 9A). Hence, increasing the delay made the neuron more sensitive, but it did not increase the saturation firing rate.

4. Discussion

4.1. Summary of the simulation results

Synchrony changes are obtained by modulating the driving current to interneuron networks. We studied firing rate modulation of a strongly coupled model network, which was representative of networks in the superficial layers of the cortex (Douglas and Martin, 2004; Yoshimura et al., 2005). Our simulations of the homogeneous, all-to-all network revealed that increasing the drive to excitatory neurons (Figure 4) had a different effect than decreasing the drive to inhibitory neurons (Figure 2). In the former case, the firing rate of excitatory and inhibitory neurons increased, typically with little changes in the delay between inhibition and excitation and in the degree of synchrony. By

contrast, when the drive to inhibitory neurons was decreased, their rate decreased, but the rate of the excitatory neurons increased. When the inhibitory neurons fired at a higher rate than the excitatory neurons, the initial difference in firing rate decreased with decreasing interneuron drive, leading to an increase in synchrony by virtue of a locking phenomenon. Decreasing interneuron drive when the network was already synchronous led to smaller changes in the rate, but the delay between inhibition and excitation increased instead. These results were robust against the effects of noise (Figure 3), sparse synaptic connectivity and heterogeneity (Figure 5). For sparse, heterogeneous networks, the mean excitatory and inhibitory rates during 1:1 locking states were not necessarily equal to the oscillation frequency. In our simulations (Figure 2Ac, 3B and 5Ab), during 1:1 locking, the oscillation frequency increased, albeit moderately, with increasing inhibitory driving current. This is not necessarily the only possibility. In other operating regions of the network, an increase in interneuron activity could lower the firing rate of the excitatory neurons, which in turn could lower the oscillation frequency.

Attentional modulation of the contrast response function. The preceding results on the modulation of synchrony and firing rate with the driving current to inhibitory and excitatory neurons were used to infer how the effects of attention could be modeled in the cortical circuit. We made the following assumptions to account for attentional modulation of the CRF. First, contrast mostly activates the excitatory neurons and to a lesser extent inhibitory neurons. Second, that interneurons fired at a higher rate than excitatory neurons. Third, that attention led to a reduction in the drive to the interneurons. This last assumption may seem counterintuitive and is discussed in the section "Model assumptions". Given the preceding assumptions, the model reproduces the following experimental observations (Figure 7 and 8). (1) Contrast leads to increases in the rates of excitatory and inhibitory cells, but does not significantly change the delay between inhibition and excitation. (2) Synchrony is only present for high contrast stimuli. (3) Attention increases the rate of excitatory cells, but decreases the rate of inhibitory cells. (4) Attention shifts the onset of synchrony to lower contrasts. Furthermore, it predicts that when there already is synchrony, attention increases the delay between inhibition and excitation. We do not claim that modulation of interneuron drive is the only way of shifting CRFs. For instance, increasing the drive to excitatory neurons or increasing the efficacy of recurrent inhibitory synapses could also lead to modulation of CRFs. We have not evaluated these possibilities within the context of the present model.

Changes in the delay between inhibition and excitation could modulate the firing rate of downstream neurons. We determined how changes in network state might affect downstream neurons (Figure 9). For the present investigation, we assumed that the downstream neuron received excitatory and inhibitory inputs from the network. Our results indicate that the changes in delay obtained from our network model could switch downstream neurons from a non-responsive to a responsive state. The response of neurons that were already responsive changed to a lesser extent. Hence, for the parameter values used here, the main effect was to increase the number of downstream neurons that are responsive to the stimulus. The changes in delay were obtained with small changes in firing rate hence, the strongest attentional modulation of firing rate may occur downstream from where attention actually modulated the driving currents to neurons.

5. Model assumptions

Representing synaptic inputs by currents. The feed-forward feature-selective and top-down modulatory inputs, as well as inputs from other neurons in the same layer but outside the network, were modeled as a time-varying current. The replacement of synaptic inputs that elicit conductance changes together with a driving current by a pure current without conductance changes is an approximation. There is disagreement about whether it is possible to get exactly the same spike train statistics with a time-varying current compared with those that are obtained for a conductance drive (Rauch et al., 2003; Rudolph and Destexhe, 2003; Richardson, 2004). Nevertheless, the mean and the variance of a current drive affect in different ways the firing rate response of an isolated neuron (Tiesinga et al., 2000; Chance et al., 2002; Fellous et al., 2003) and the coherence of a network (Tiesinga and José, 2000). When the input rate of synaptic inputs is increased, it increases the mean as well as the variance of the current. Here we used a current drive, so that we could independently vary the mean and variance in the simplest possible way. When the mean and variance were co-varied to represent increasing the rate of synaptic inputs, synchrony and delay modulations similar to those reported here were obtained (results not shown).

Can attention reduce the drive to the interneurons? Attention has been associated with activation of cholinergic projections (Hasselmo and McGaughy, 2004; Coull, 2005; Milstein et al., 2005; Sarter et al., 2005). Cholinergic effects mediated through the M1 receptor are excitatory, because they inhibit a voltage-sensitive K+ channel. In contrast,

effects mediated through the M2 and M4 receptor are inhibitory because acetylcholine activates an inward rectifying K+channel (Feldman et al., 1997). The M1, M2 and M4 receptors are all expressed in the neocortex (Feldman et al., 1997). However, in the neocortex, acetylcholine is generally thought to have excitatory effects on neurons (Krnjevic, 1993). How can it cause the drive to the interneurons to decrease? There are at least two possible mechanisms. There could be a second set of interneurons that is activated by attention, these neurons might inhibit the interneurons studied here, thus reducing their rate (Wang et al., 2004). There are multiple, functionally distinct networks of interneurons in cortex that could play this role (Beierlein et al., 2003; Markram et al., 2004). Cortical interneurons have been classified based either on their physiological characteristics, or on their morphological characteristics or sometimes based on their neurochemical characteristics. The link between the results of different classification methods has not been conclusively established. We speculate that the second set of neurons may either consist of interneurons that are physiologically classified as low threshold spiking (LTS), since these are more sensitive to neuromodulators than fast spiking interneurons (Beierlein et al., 2003), or those that are morphologically classified as interneuron targeting cells (and contain the calcium binding protein calbindin) (Markram et al., 2004; Wang et al., 2004). The levels of muscarinic receptor expression varies across brain areas, M1 is expressed at the highest level in the neocortex, whereas M2 is expressed at the highest level in the cerebellum (Feldman et al., 1997). This would seem to suggest that the expression of receptors can be tightly controlled, hence, that it could be cell-type specific, with one type of interneuron more sensitive to a specific neuromodulator than the other. For instance, the interneurons in the model network could be inhibited, or even not affected at all, by acetylcholine, whereas the postulated second set of interneurons are excited by acetylcholine. Another possibility, suggested by measurements on recurrent excitatory synapses in the hippocampus (Hasselmo et al., 1995), is that acetylcholine reduces the efficacy of excitatory synapses onto inhibitory cells. The synaptic strength is modulated by acetylcholine via autoreceptors on the presynaptic neuron (Cooper JR, 1996). Hence, if excitatory synapses onto excitatory neurons are modulated by acetylcholine (Hasselmo et al., 1995; Hasselmo and McGaughy, 2004; Sarter et al., 2005), it could also be the case that those onto inhibitory neurons are similarly modulated. The converse could also be true, since it was shown that inhibitory synapses could have different facilitation and depression properties based on their postsynaptic target (Gupta et al., 2000). Hence, this issue needs to be resolved experimentally.

5.1. Comparison to previous theoretical studies.

Previous theoretical studies and model simulations have shown that interneuron networks can be made to synchronize in the gamma-frequency range (Whittington et al., 1995; Wang and Buzsáki, 1996; Golomb and Hansel, 2000; Tiesinga and José, 2000; Bartos et al., 2001; Aradi and Soltesz, 2002; Bartos et al., 2002; Olufsen et al., 2003). The synchronization is robust against heterogeneity in the physiological properties of the interneurons (Wang and Buzsáki, 1996; White et al., 1998), noisy background activity (Tiesinga and José, 2000) and sparse connectivity (Wang and Buzsáki, 1996; Golomb and Hansel, 2000; Borgers and Kopell, 2003). In other investigations it was found that there are two mechanisms for obtaining gamma frequency oscillations in mixed excitatory-inhibitory networks (Bush and Sejnowski, 1996; Tiesinga et al., 2001; Borgers and Kopell, 2003; Brunel and Wang, 2003; Hansel and Mato, 2003; Borgers and Kopell, 2005; Borgers et al., 2005). In the first mechanism, the sparsely firing excitatory cells are entrained to the periodic inhibition produced by the synchronized interneuron network. This mechanism is referred to as interneuron gamma (ING) (Whittington et al., 2000). In the second mechanism, the activity of excitatory neurons recruits interneurons, which in turn temporarily shuts off the excitatory neurons, after which the whole process repeats itself. This mechanism is known as pyramidal-interneuron gamma (PING) (Whittington et al., 2000). The focus of the present investigation differs from the preceding ones. We address two issues. First, is it possible to vary the degree of synchrony without significantly affecting the firing rate of excitatory and inhibitory neurons? Second, can the degree of synchrony be modulated on rapid time scales? Previously, we addressed these issues for an isolated interneuron network (Tiesinga and Sejnowski, 2004). Here, we find that the degree of synchrony and the delay between inhibition and excitation, can be modulated dynamically in a mixed excitatory-inhibitory network with only minor changes in the neurons' firing rate. The model used in this paper and the cited papers are far too simple to account for the detailed dynamics of a cortical column. Our goal is to use the present model as a part of a much larger - 1000 or more columns - model of the visual cortex. Therefore we had to make some simplifications to make the calculations feasible. A different line of research is to include more ionic channels, use multicompartmental single neuron models and account for more distinct types of neurons. A recent example is the work by Traub and coworkers (Traub et al., 2005).

Modulation of delay between inhibition and excitation and models for stimulus competition. When two visual stimuli are presented si-

multaneously, the corresponding neural activity patterns may compete for control of neurons in downstream areas (Desimone and Duncan, 1995). In a recent paper it was argued that synchronous inhibition could help with this stimulus competition (Borgers et al., 2005). The authors proposed that a strong stimulus (the winner) would spike the responding neurons before the synchronous inhibition arrives and the neurons responding to the weak stimulus (the loser) would be prevented from spiking by the inhibition. In this way the inhibition only affects the activity of the loser. By contrast, tonic inhibition would affect both the winner and loser equally. Here we propose that attention can increase the delay between inhibition and excitation: this would make it harder to stop a weak stimulus that spikes neurons immediately after the spikes of neurons responding to the strong stimulus. The two models are not in conflict because they speak to different situations. First, our model is meant to represent one cortical column, rather than multiple columns that compete. Second, the downstream effects in our model are vertical, from layer 4 to layer 2/3 and from layer 2/3 to layer 5, rather than horizontal. Further theoretical studies are necessary to properly integrate the vertical and horizontal components of attention.

5.2. Comparison to experimental results and future work

Response versus contrast gain. The model could account for shifts in the CRF with attention observed for V4 neurons by (Reynolds et al., 2000; Reynolds and Desimone, 2003). Their results provide support for a contrast gain model rather than a response gain model. However, in other experiments (McAdams and Maunsell, 1999), where a neuron's orientation tuning curve was measured, it was concluded that the response gain model was a more appropriate description. These two experiments are not directly comparable because the behavioral task was different and the responses in (McAdams and Maunsell, 1999) may not have reached contrast-saturation. In addition, varying stimulus orientation alters the identity of the cortical neurons that drive the neuron, whereas contrast does not, rather it increases the rate of the neurons providing input. As a result, properties, such as neural synchrony, are modulated differently by contrast compared with orientation (Kohn and Smith, 2005). Further experimental studies of the modulation of firing rate with attention, luminance contrast and the value of stimulus features are needed (Reynolds and Chelazzi, 2004).

Synchrony modulation and contrast. In experiments conducted to measure attentional modulation of synchrony, the stimulus is presented for a long time (Fries et al., 2001; Taylor et al., 2005), on the order of seconds, whereas contrast-response curves are usually obtained using

short 50-250 ms stimuli (Reynolds and Desimone, 2003). Hence, it may not be appropriate to directly compare these experimental results. To the best of our knowledge, there are no experiments in which the attentional modulation of the synchrony-versus-contrast curves was measured directly. Previous studies did, however, address the relation between gamma-frequency oscillations, stimulus orientation and contrast. Here we briefly summarize these studies. Gamma-frequency oscillations could be measured in recordings from feline and primate primary visual cortex when the stimulus was close to optimal in terms of the cell's preferred orientation, it had a high contrast and it was large (Gray and Viana Di Prisco, 1997). In macaque V1 it was found that the spectral content of the local field potential in the gamma-frequency range increased with contrast (Henrie and Shapley, 2005). The oscillatory synchrony is stimulus specific and is absent or very weak during spontaneous activity (Gray and Viana Di Prisco, 1997). The gamma oscillations were localized on the cortical surface; only those areas that responded to the region of visual field where the stimulus was located were synchronized (Rols et al., 2001). The degree of synchrony was tuned for stimulus orientation and it increased with contrast (Gray and Viana Di Prisco, 1997). Furthermore, frequency bands of the LFP power spectrum were tuned for orientation, and spatial and temporal frequency (Kayser and Konig, 2004). Even the oscillation frequency itself could depend on stimulus features. For instance, when the speed of a moving stimulus bar was increased, the oscillation frequency also increased (Gray and Viana Di Prisco, 1997). The preceding results show that synchrony and rate modulations produced by the model could be feasible. However, further experiments are needed to determine how the synchrony-versus-contrast curves are modulated by attention. Our simulation results predict that there should be a group of interneurons that lower their rate with attention. It is therefore key to record from identified cortical interneurons in awake animals, which is challenging from an experimental point of view (Constantinidis and Goldman-Rakic, 2002; Swadlow, 2003).

Acknowledgements

Appendix

A. The model equations

Interneuron model

The interneuron was modeled as a single compartment with Hodgkin-Huxley-type voltage-gated sodium and potassium currents and a passive leak current (Wang and Buzsáki, 1996). The equation for the membrane potential of the model neuron is:

$$C_m \frac{dV}{dt} = -I_{Na} - I_K - I_L - I_{GABA} - I_{AMPA} + I + C_m \xi$$

where $I_L = g_L(V - E_L)$ is the leak current, $I_{Na} = g_{Na} m_\infty^3 h (V - E_{Na})$ is the sodium current, $I_K = g_K n^4 (V - E_K)$ is the potassium current, I_{GABA} is the inhibitory synaptic current and I_{AMPA} is the excitatory synaptic current. The Gaussian noise variable is denoted with ξ while I is the tonic drive. The gating variables are given in terms of m, n, and h and they satisfy the equation

$$\frac{dx}{dt} = \zeta(\alpha_x(1 - x) - \beta_x)$$

Here the label x stands for the kinetic variable, and $\zeta = 5$ is a dimensionless time scale that can be used to tune the temperature dependent speed with which the channels open or close. The rate constants are:

$$\alpha_m = \frac{-0.1(V + 35)}{\exp(-0.1(V + 35)) - 1}, \quad \beta_m = 4\exp(-(V + 60)/18)$$

$$\alpha_h = 0.07\exp(-(V + 58)/20), \quad \beta_h = \frac{1}{\exp(-0.1(V + 28)) + 1}$$

$$\alpha_n = \frac{-0.01(V + 34)}{\exp(-0.1(V + 34)) - 1}, \quad \beta_n = 0.125\exp(-(V + 44)/80)$$

and the asymptotic values of the gating variables are:

$$x_\infty(V) = \frac{\alpha_x}{\alpha_x + \beta_x}$$

where x stands for m, n, and h. We made the approximation that m follows the asymptotic value $m_\infty(V)$ instantaneously (Wang and Buzsáki, 1996).

Pyramidal neuron model

A different single compartment Hodgkin-Huxley-type model was used for the dynamics of the pyramidal neuron (Golomb and Amitai, 1997). The membrane potential obeys the following differential equation:

$$C_m\frac{\mathrm{d}V}{\mathrm{d}t} = -I_{Na} - I_{NaP} - I_K - I_{Kdr} - I_{KA} - I_{Kslow}$$
$$-I_L - I_{GABA} - I_{AMPA} + I + C_m\xi$$

where $I_L = g_L(V - E_L)$ is the leak current, $I_{Na} = g_{Na}m_\infty^3 h(V - E_{Na})$ is the sodium current, $I_{NaP} = g_{NaP}p_\infty h(V - E_{Na})$ is the persistent sodium current, $I_{Kdr} = g_{Kdr}n^4(V - E_K)$ is the delayed rectifier potassium current, $I_{KA} = g_{KA}a_\infty^3 b(V - E_K)$ is the A-type potassium current, $I_{Kslow} = g_{Kslow}z(V - E_K)$ is the slow potassium current, I_{GABA} is the inhibitory synaptic current and I_{AMPA} is the excitatory synaptic current. The Gaussian noise variable is denoted by ξ while I is the tonic drive. The kinetic variables h, n, b and z satisfy the equation

$$\frac{\mathrm{d}x}{\mathrm{d}t} = \frac{x_\infty(V) - x}{\tau_x}$$

The rate constants are:

$$
\begin{aligned}
m_\infty &= [\exp(-(V + 30)/9.5) + 1]^{-1} \\
h_\infty &= [\exp((V + 53)/7) + 1]^{-1} \\
\tau_h &= 0.37 + 2.78 \times [\exp((V + 40.5)/6) + 1]^{-1} \\
p_\infty &= [\exp(-(V + 40)/5) + 1]^{-1} \\
n_\infty &= [\exp(-(V + 30)/10) + 1]^{-1} \\
\tau_n &= 0.37 + 1.85 \times [\exp((V + 27)/15) + 1]^{-1} \\
a_\infty &= [\exp(-(V + 50)/20) + 1]^{-1} \\
b_\infty &= [\exp((V + 80)/6) + 1]^{-1} \\
\tau_b &= 15\,\mathrm{ms} \\
z_\infty &= [\exp((V + 80)/6) + 1]^{-1} \\
\tau_z &= 15\,\mathrm{ms}
\end{aligned}
$$

The fast gating variables m, p and a instantaneously followed their asymptotic value m_∞, p_∞ and a_∞, respectively. The standard set of parameter values used in this paper is:

Parameter (units)	Pyramidal Neurons	Interneurons
E_L (mV)	-70	-65
E_{Na} (mV)	55	55
E_K (mV)	-90	-90
E_{AMPA} (mV)	0	0
E_{GABA} (mV)	-75	-75
g_L (mS/cm^2)	0.02	0.1
g_{Na} (mS/cm^2)	24	35
g_{NaP} (mS/cm^2)	0.07	-
g_{Kdr} (mS/cm^2)	3	-
g_{KA} (mS/cm^2)	1.4	-
g_{Kslow} (mS/cm^2)	1	-
g_K (mS/cm^2)	-	9
C_m (μF/cm^2)	1	1

The initial values of the membrane potential at the beginning of the simulation were chosen randomly from a uniform distribution between -70 mV and -50 mV. The gating variables were set to their asymptotic stationary values, x_∞, corresponding to the starting value, V, of the membrane potential.

The tonic drive, I, for excitatory (inhibitory) neurons, was the sum of a common component I_{exc} (I_{inh}) and a heterogeneous component that varied across neurons with a variance σ^2_{exc} (σ^2_{inh}). The common component was varied on a two-dimensional grid of current values in the range $-2 < I_{inh} < 1$ μA/cm^2 and $1 < I_{exc} < 6$ μA/cm^2. The Gaussian synaptic noise ξ_i in the current of neuron i is chosen such that $\langle i(t) \rangle = 0$ and $\langle i(t) \rangle = 2\lambda\delta(t - t')\delta_{ij}$. On each integration time step, the noise was drawn independently from a distribution between $-\sqrt{6\lambda/dt}$ and $\sqrt{6\lambda/dt}$, where dt was the time step. The differential equations are integrated using a second-order Runge-Kutta method with a time step of $dt = 0.01$ ms or 0.05 ms (Gerald and Wheatley, 1999; Press et al., 1992).

Synaptic models

Each synapse is modeled using a gating variable s_{ji}, with j being the index of the postsynaptic neuron and i being the index of the presynaptic neuron. Since there are no synaptic delays or synaptic failures in our model, the gating variables for synapses originating from the same presynaptic neuron will have the same value: $s_{ji} = s_i$. Furthermore, because the connectivity is all-to-all, the sum across gating variables of all the synapses impinging on postsynaptic neuron j is the same for each neuron:

$$\sum_{i(j)} s_{ji} = \sum_i s_i \equiv s_{tot}$$

Here $i(j)$ stands for all neurons i that project to neuron j. Hence, we need to calculate it only once for all the excitatory and once for all the inhibitory synapses. This resulted in a significant speed up of the computation. s_i^{inh} and s_i^{exc} are the gating variables for the inhibitory and excitatory synapses, respectively. The synapses were labeled by the presynaptic neuron i. The synaptic gating variables obey the following equation:

$$\frac{\mathrm{d}s_i^{exc}}{\mathrm{d}t} = \frac{1}{\tau^{exc}(k^{exc}\sum_k \delta(t - t_k^i) - s^{exc})} \tag{1}$$

$$\frac{\mathrm{d}s_i^{inh}}{\mathrm{d}t} = \frac{1}{\tau^{inh}(k^{inh}\sum_k \delta(t - t_k^i) - s^{inh})} \tag{2}$$

where t_k^i is the kth spike time generated by the ith neuron, $\tau^{exc} = 5$ ms, $\tau^{inh} = 10$ ms are the synaptic decay times for excitatory and inhibitory synapses, respectively. For the sparse, heterogenous network we used $\tau^{exc} = 2$ ms, $\tau^{inh} = 8$ ms instead. We used a sum of Dirac delta functions to account for the arrival of the spikes to the postsynaptic neuron, because it was computationally less expensive. In (Golomb and Amitai, 1997; Wang and Buzsáki, 1996) the equation for the gating variable is written in the form:

$$\frac{\mathrm{d}s}{\mathrm{d}t} = \alpha F(V_{pre})(1 - s) - \beta s \tag{3}$$

where F represents the normalized concentration of the postsynaptic transmitter-receptor complex and is assumed to be an instantaneous sigmoid function of the presynaptic membrane potential V_{pre} :

$$F(V_{pre}) = \frac{1}{1 + \exp(-(V_{pre} - \theta_s)/\sigma_s)} \tag{4}$$

θ_s is the voltage threshold for synaptic release and takes the value 0 mV for interneurons and -20 mV for pyramidal neurons, and $\sigma_s = 2$ mV. The constants $k_{exc} = 0.44$ and $k_{inh} = 1$ in our formulation were determined by fitting the result of eqns (1) and (2) to the result produced by (3) and (4). The synaptic currents take the values:

$$
\begin{aligned}
I_{GABA}^{exc} &= \frac{g_{ie}}{N_{ie}} s_{tot}^{inh}(t)(V - E_{GABA}) \\
I_{AMPA}^{exc} &= \frac{g_{ee}}{N_{ee}} s_{tot}^{exc}(t)(V - E_{AMPA}) \\
I_{GABA}^{inh} &= \frac{g_{ii}}{N_{ii}} s_{tot}^{inh}(t)(V - E_{GABA}) \\
I_{AMPA}^{inh} &= \frac{g_{ei}}{N_{ei}} s_{tot}^{exc}(t)(V - E_{AMPA})
\end{aligned}
$$

where g_{ee} is the conductance of the excitatory synapses onto the excitatory neurons, g_{ie} is the conductance of the inhibitory synapses onto the excitatory neurons, g_{ei} is the conductance of the excitatory synapses onto the inhibitory neurons and g_{ii} is the conductance of inhibitory synapses onto the inhibitory neurons. N_{ie} is the number of inhibitory synapses on excitatory neurons, the quantities N_{ei}, N_{ii}, N_{ee} are defined analogously. For the all-to-all network, $N_{ie} = N_{ii} = N_{inh}$ and $N_{ei} = N_{ee} = N_{exc}$, here N_{exc} is the number of excitatory neurons and N_{inh} is the number of inhibitory neurons. For the sparsely connected network, $N_{ie} = 0.2N_{inh}$, $N_{ii} = N_{inh}$, $N_{ei} = N_{ee} = 0.2N_{exc}$. In this case s_{tot} is the sum over all the presynaptic neurons that provide input to the postsynaptic neuron, hence, its value does depend on the identity of the postsynaptic neuron. The actual coupling parameters are listed in the Methods.

References

Albrecht, D., W. Geisler, R. Frazor, and A. Crane: 2002, 'Visual cortex neurons of monkeys and cats: temporal dynamics of the contrast response function'. *J Neurophysiol* **88**, 888–913.

Albrecht, D. and D. Hamilton: 1982, 'Striate cortex of monkey and cat: contrast response function'. *J Neurophysiol* **48**, 217–237.

Alitto, H. and W. Usrey: 2004, 'Influence of contrast on orientation and temporal frequency tuning in ferret primary visual cortex'. *J Neurophysiol* **91**, 2797–2808.

Aradi, I. and I. Soltesz: 2002, 'Modulation of network behaviour by changes in variance in interneuronal properties'. *J Physiol* **538**, 227–251.

Bartos, M., I. Vida, M. Frotscher, J. Geiger, and P. Jonas: 2001, 'Rapid signaling at inhibitory synapses in a dentate gyrus interneuron network'. *J Neurosci* **21**, 2687–2698.

Bartos, M., I. Vida, M. Frotscher, A. Meyer, H. Monyer, J. Geiger, and P. Jonas: 2002, 'Fast synaptic inhibition promotes synchronized gamma oscillations in hippocampal interneuron networks'. *Proc Natl Acad Sci U S A* **99**, 13222–13227.

Beierlein, M., J. Gibson, and B. Connors: 2003, 'Two Dynamically Distinct Inhibitory Networks in Layer 4 of the Neocortex'. *Journal of Neurophysiology* **90**, 2987–3000.

Bichot, N., A. Rossi, and R. Desimone: 2005, 'Parallel and serial neural mechanisms for visual search in macaque area V4'. *Science* **308**, 529–534.

Binzegger, T., R. Douglas, and K. Martin: 2004, 'A quantitative map of the circuit of cat primary visual cortex'. *J Neurosci* **24**, 8441–8453.

Blasdel, G.: 1992a, 'Differential imaging of ocular dominance and orientation selectivity in monkey striate cortex'. *J Neurosci* **12**, 3115–3138.

Blasdel, G.: 1992b, 'Orientation selectivity, preference, and continuity in monkey striate cortex'. *J Neurosci* **12**, 3139–3161.

Borgers, C., S. Epstein, and N. Kopell: 2005, 'Background gamma rhythmicity and attention in cortical local circuits: A computational study'. *Proc Natl Acad Sci U S A* **102**, 7002–7007.

Borgers, C. and N. Kopell: 2003, 'Synchronization in networks of excitatory and inhibitory neurons with sparse, random connectivity'. *Neural Comput* **15**, 509–538.

Borgers, C. and N. Kopell: 2005, 'Effects of noisy drive on rhythms in networks of excitatory and inhibitory neurons'. *Neural Comput* **17**, 557–608.

Brunel, N. and V. Hakim: 1999, 'Fast global oscillations in networks of integrate-and-fire neurons with low firing rates'. *Neural Comput* **11**, 1621–1671.

Brunel, N. and X. Wang: 2003, 'What determines the frequency of fast network oscillations with irregular neural discharges? I. Synaptic dynamics and excitation-inhibition balance'. *Journal of Neurophysiology* **90**, 415–430.

Bush, P. and T. Sejnowski: 1996, 'Inhibition synchronizes sparsely connected cortical neurons within and between columns in realistic network models'. *J Comput Neurosci* **3**, 91–110.

Callaway, E.: 1998, 'Local circuits in primary visual cortex of the macaque monkey'. *Annu Rev Neurosci* **21**, 47–74.

Chance, F., L. Abbott, and A. Reyes: 2002, 'Gain modulation from background synaptic input'. *Neuron* **35**, 773–782.

Constantinidis, C. and P. Goldman-Rakic: 2002, 'Correlated discharges among putative pyramidal neurons and interneurons in the primate prefrontal cortex'. *J Neurophysiol* **88**, 3487–3497.

Cooper JR, Bloom FE, R. R.: 1996, *The biochemical basis of neuropharmacology*. Oxford: Oxford University Press, 7th edition edition.

Coull, J.: 2005, 'Psychopharmacology of human attention'. In: T. J. Itti L, Rees G (ed.): *Neurobiology of Attention*. San Diego: Elsevier Academic Press, pp. 50–56.

Desimone, R. and J. Duncan: 1995, 'Neural mechanisms of selective visual attention'. *Annu Rev Neurosci* **18**, 193–222.

Douglas, R. and K. Martin: 2004, 'Neuronal circuits of the neocortex'. *Annu Rev Neurosci* **27**, 419–451.

Feldman, R., J. Meyer, and L. Quenzer: 1997, *Principles of Neuropsychopharmacology*. Sunderland, Massachusetts: Sinauer Associates.

Fellous, J., M. Rudolph, A. Destexhe, and T. Sejnowski: 2003, 'Synaptic background noise controls the input/output characteristics of single cells in an in vitro model of in vivo activity'. *Neuroscience* **122**, 811–829.

Fries, P., J. Reynolds, A. Rorie, and R. Desimone: 2001, 'Modulation of oscillatory neuronal synchronization by selective visual attention'. *Science* **291**, 1560–1563.

Geisler, C., N. Brunel, and W. XJ: 2005, 'Contributions of intrinsic membrane dynamics to fast network oscillations with irregular neuronal discharges'. *J Neurophysiol.*

Gerald, C. and P. Wheatley: 1999, *Applied Numerical Analysis*. Reading, California: Addison-Wesley, 6th edition edition.

Ghose, G. and D. Ts'o: 1997, 'Form processing modules in primate area V4'. *J Neurophysiol* **77**, 2191–2196.

Golomb, D. and Y. Amitai: 1997, 'Propagating Neuronal Discharges in Neocortical Slices: Computational and Experimental Study'. *J. Neurophysiol.* **78**, 1199–1211.

Golomb, D. and D. Hansel: 2000, 'The number of synaptic inputs and the synchrony of large, sparse neuronal networks'. *Neural Comput* **12**, 1095–1139.

Gray, C. and G. Viana Di Prisco: 1997, 'Stimulus-dependent neuronal oscillations and local synchronization in striate cortex of the alert cat'. *J Neurosci* **17**, 3239–3253.

Gupta, A., Y. Wang, and H. Markram: 2000, 'Organizing principles for a diversity of GABAergic interneurons and synapses in the neocortex'. *Science* **287**, 273–278.

Hansel, D. and G. Mato: 2003, 'Asynchronous states and the emergence of synchrony in large networks of interacting excitatory and inhibitory neurons'. *Neural Comput* **15**, 1–56.

Hansel, D. and C. van Vreeswijk: 2002, 'How noise contributes to contrast invariance of orientation tuning in cat visual cortex'. *J Neurosci* **22**, 5118–5128.

Hasselmo, M. and J. McGaughy: 2004, 'High acetylcholine levels set circuit dynamics for attention and encoding and low acetylcholine levels set dynamics for consolidation'. *Prog Brain Res* **145**, 207–231.

Hasselmo, M., E. Schnell, and E. Barkai: 1995, 'Dynamics of learning and recall at excitatory recurrent synapses and cholinergic modulation in rat hippocampal region CA3'. *J Neurosci* **15**, 5249–5262.

Henrie, J. and R. Shapley: 2005, 'LFP power spectra in V1 cortex: the graded effect of stimulus contrast'. *J Neurophysiol.*

Hubel, D.: 1959, 'Single unit activity in striate cortex of unrestrained cats'. *J Physiol* **147**, 226–238.

Hubel, D. and T. Wiesel: 1959, 'Receptive fields of single neurones in the cat's striate cortex'. *J Physiol* **148**, 574–591.

Hubel, D. and T. Wiesel: 1962, 'Receptive fields, binocular interaction and functional architecture in the cat's visual cortex'. *J Physiol* **160**, 106–154.

Kayser, C. and P. Konig: 2004, 'Stimulus locking and feature selectivity prevail in complementary frequency ranges of V1 local field potentials'. *Eur J Neurosci* **19**, 485–489.

Kohn, A. and M. Smith: 2005, 'Stimulus dependence of neuronal correlation in primary visual cortex of the macaque'. *J Neurosci* **25**, 3661–3673.

Krnjevic, K.: 1993, 'Central cholinergic mechanisms and function'. *Prog Brain Res* **98**, 285–292.

Luck, S., L. Chelazzi, S. Hillyard, and R. Desimone: 1997, 'Neural mechanisms of spatial selective attention in areas V1, V2, and V4 of macaque visual cortex'. *J Neurophysiol* **77**, 24–42.

Markram, H., M. Toledo-Rodriguez, Y. Wang, A. Gupta, G. Silberberg, and C. Wu: 2004, 'Interneurons of the neocortical inhibitory system'. *Nat Rev Neurosci* **5**, 793–807.

McAdams, C. and J. Maunsell: 1999, 'Effects of attention on orientation-tuning functions of single neurons in macaque cortical area V4'. *J Neurosci* **19**, 431–441.

Miller, K. and T. Troyer: 2002, 'Neural noise can explain expansive, power-law nonlinearities in neural response functions'. *J Neurophysiol* **87**, 653–659.

Milstein, J., J. Dalley, and R. TW: 2005, 'Neuropharmacology of Attention'. In: T. J. Itti L, Rees G (ed.): *Neurobiology of Attention*. San Diego: Elsevier Academic Press, pp. 57–62.

Moran, J. and R. Desimone: 1985, 'Selective attention gates visual processing in the extrastriate cortex'. *Science* **229**, 782–784.

Ohzawa, I., G. Sclar, and R. Freeman: 2002, 'Contrast gain control in the cat visual cortex'. *Nature* **298**, 266–268.

Olufsen, M., M. Whittington, M. Camperi, and N. Kopell: 2003, 'New roles for the gamma rhythm: population tuning and preprocessing for the Beta rhythm'. *J Comput Neurosci* **14**, 33–54.

Press, W., S. Teukolsky, W. Vetterling, and B. Flannery: 1992, *Numerical Recipes*. Cambridge: Cambridge University Press.

Rauch, A., G. La Camera, H. Luscher, W. Senn, and S. Fusi: 2003, 'Neocortical pyramidal cells respond as integrate-and-fire neurons to in vivo-like input currents'. *J Neurophysiol* **90**, 1598–1612.

Reynolds, J. and L. Chelazzi: 2004, 'Attentional modulation of visual processing'. *Annual Review of Neuroscience* **27**, 611–647.

Reynolds, J. and R. Desimone: 2003, 'Interacting roles of attention and visual salience in V4'. *Neuron* **37**, 853–863.

Reynolds, J., T. Pasternak, and R. Desimone: 2000, 'Attention increases sensitivity of V4 neurons'. *Neuron* **26**, 703–714.

Richardson, M.: 2004, 'Effects of synaptic conductance on the voltage distribution and firing rate of spiking neurons'. *Phys Rev E Stat Nonlin Soft Matter Phys* **69**, 051918.

Rols, G., C. Tallon-Baudry, P. Girard, O. Bertrand, and J. Bullier: 2001, 'Cortical mapping of gamma oscillations in areas V1 and V4 of the macaque monkey'. *Vis Neurosci* **18**, 527–540.

Rudolph, M. and A. Destexhe: 2003, 'The discharge variability of neocortical neurons during high-conductance states'. *Neuroscience* **119**, 855–873.

Salin, P. and J. Bullier: 1995, 'Corticocortical connections in the visual system: structure and function'. *Physiol Rev* **75**, 107–154.

Salinas, E. and T. Sejnowski: 2000, 'Impact of correlated synaptic input on output variability in simple neuronal models'. *J Neurosci* **20**, 6193–6209.

Sarter, M., M. Hasselmo, J. Bruno, and B. Givens: 2005, 'Unraveling the attentional functions of cortical cholinergic inputs: interactions between signal-driven and cognitive modulation of signal detection'. *Brain Res Brain Res Rev* **48**, 98–111.

Sclar, G. and R. Freeman: 1982, 'Orientation selectivity in the cat's striate cortex is invariant with stimulus contrast'. *Exp Brain Res* **46**, 457–461.

Shepherd, G., A. Stepanyants, I. Bureau, D. Chklovskii, and K. Svoboda: 2005, 'Geometric and functional organization of cortical circuits'. *Nat Neurosci* **8**, 782–790.

Song, S., P. Sjostrom, M. Reigl, S. Nelson, and D. Chklovskii: 2005, 'Highly non-random features of synaptic connectivity in local cortical circuits'. *PLoS Biol* **3**, e68.

Swadlow, H.: 2003, 'Fast-spike Interneurons and Feedforward Inhibition in Awake Sensory Neocortex'. *Cereb Cortex* **13**, 25–32.

Taylor, K., S. Mandon, W. Freiwald, and A. Kreiter: 2005, 'Coherent Oscillatory Activity in Monkey Area V4 Predicts Successful Allocation of Attention'. *Cereb Cortex.*

Tiesinga, P., J. Fellous, J. Jose, and T. Sejnowski: 2001, 'Computational model of carbachol-induced delta, theta, and gamma oscillations in the hippocampus'. *Hippocampus* **11**, 251–274.

Tiesinga, P., J.-M. Fellous, E. Salinas, J. Jose, and T. Sejnowski: 2004a, 'Inhibitory synchrony as a mechanism for attentional gain modulation'. *J Physiol (Paris)* **98**, 296–314.

Tiesinga, P., J.-M. Fellous, E. Salinas, J. José, and T. Sejnowski: 2004b, 'Synchronization as a mechanism for attentional gain modulation'. *Neurocomputing* **58-60**, 641–646.

Tiesinga, P. and J. José: 2000, 'Robust gamma oscillations in networks of inhibitory hippocampal interneurons'. *Network* **11**, 1–23.

Tiesinga, P., J. Jose, and T. Sejnowski: 2000, 'Comparison of current-driven and conductance-driven neocortical model neurons with Hodgkin-Huxley voltage-gated channels'. *Physical Review E* **62**, 8413–8419.

Tiesinga, P. and T. Sejnowski: 2004, 'Rapid temporal modulation of synchrony by competition in cortical interneuron networks'. *Neural Computation* **16**, 251–275.

Traub, R., D. Contreras, M. Cunningham, H. Murray, F. LeBeau, A. Roopun, A. Bibbig, W. Wilent, M. Higley, and W. MA: 2005, 'Single-column thalamocortical network model exhibiting gamma oscillations, sleep spindles, and epileptogenic bursts'. *J Neurophysiol* **93**, 2194–2232.

Troyer, T., A. Krukowski, N. Priebe, and K. Miller: 1998, 'Contrast-invariant orientation tuning in cat visual cortex: thalamocortical input tuning and correlation-based intracortical connectivity'. *J Neurosci* **18**, 5908–5927.

Wang, X. and G. Buzsáki: 1996, 'Gamma oscillation by synaptic inhibition in a hippocampal interneuronal network model'. *J. Neurosci.* **16**, 6402–6413.

Wang, X., J. Tegner, C. Constantinidis, and P. Goldman-Rakic: 2004, 'Division of labor among distinct subtypes of inhibitory neurons in a cortical microcircuit of working memory'. *Proc Natl Acad Sci U S A* **101**, 1368–1373.

White, J., C. Chow, J. Ritt, C. Soto-Trevino, and N. Kopell: 1998, 'Synchronization and oscillatory dynamics in heterogeneous, mutually inhibited neurons'. *J Comput Neurosci* **5**, 5–16.

Whittington, M., R. Traub, and J. Jefferys: 1995, 'Synchronized oscillations in interneuron networks driven by metabotropic glutamate receptor activation'. *Nature* **373**, 612–615.

Whittington, M., R. Traub, N. Kopell, B. Ermentrout, and E. Buhl: 2000, 'Inhibition-based rhythms: experimental and mathematical observations on network dynamics'. *Int J Psychophysiol* **38**, 315–336.

Yoshimura, Y., J. Dantzker, and E. Callaway: 2005, 'Excitatory cortical neurons form fine-scale functional networks'. *Nature* **433**, 868–873.